Science of the Total Environment 775 (2021) 145860

Contents lists available at ScienceDirect

Science of the Total Environment

journal homepage: www.elsevier.com/locate/scitotenv

Warmer springs have increased the frequency and extension of late-frost defoliations in southern European beech forests

Gabriel Sangüesa-Barreda [a,*], Alfredo Di Filippo [b], Gianluca Piovesan [b], Vicente Rozas [a], Luca Di Fiore [b], Miguel García-Hidalgo [a], Ana I. García-Cervigón [c], Diego Muñoz-Garachana [a], Michele Baliva [b], José M. Olano [a]

[a] EiFAB-iuFOR, University of Valladolid, Campus Duques de Soria, 42004 Soria, Spain
[b] Department of Agriculture and Forest Sciences (DAFNE), University of Tuscia, Viterbo, Italy
[c] Biodiversity and Conservation Area, Rey Juan Carlos University, c/Tulipán s/n, E-28933 Móstoles, Spain

HIGHLIGHTS

- Earlier leaf phenology by warmer springs may boost late frost defoliation (LFD).
- We reconstructed LFD events since 1950 in southern *Fagus sylvatica* distribution.
- Drier and higher populations suffer more LFD events.
- LFD events frequency has increased at the southernmost beech forests.
- Recent LFD events have larger geographical extent.

GRAPHICAL ABSTRACT

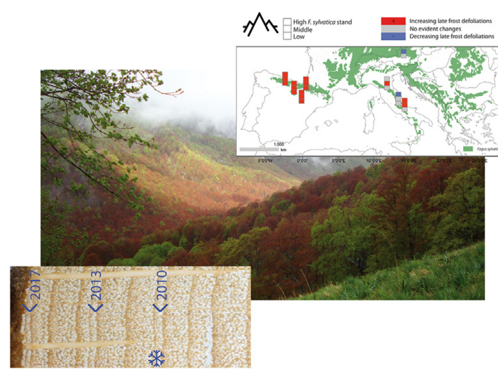

ARTICLE INFO

Article history:
Received 23 October 2020
Received in revised form 10 February 2021
Accepted 10 February 2021
Available online 13 February 2021

Editor: Elena Paoletti

Keywords:
Basal area increment
Fagus sylvatica
Late spring frost defoliation
Mixed-effect model
Tree-rings
Warm springs

ABSTRACT

Climate change is increasing the frequency of extreme climate events, causing profound impacts on forest function and composition. Late frost defoliation (LFD) events, the loss of photosynthetic tissues due to low temperatures at the start of the growing season, might become more recurrent under future climate scenarios. Therefore, the detection of changes in late-frost risk in response to global change emerges as a high-priority research topic. Here, we used a tree-ring network from southern European beech (*Fagus sylvatica* L.) forests comprising Spain, Italy and the Austrian Alps, to assess the incidence of LFD events in the last seven decades. We fitted linear-mixed models of basal area increment using different LFD indicators considering warm spring temperatures and late-spring frosts as fixed factors. We reconstructed major LFD events since 1950, matching extreme values of LFD climatic indicators with sharp tree-ring growth reductions. The last LFD events were validated using remote sensing. Lastly, reconstructed LFD events were climatically and spatially characterized. Warm temperatures before the late-spring frost, defined by high values of growing-degree days, influenced beech growth negatively, particularly in the southernmost populations. The number of LFD events increased towards beech southern distribution edge. Spanish and the southernmost Italian beech forests experienced higher frequency of LFD events since the 1990s. Until then, LFD events were circumscribed to local scales, but since that decade, LFD events became widespread, largely affecting the whole beech southwestern distribution area. Our study, based on in-situ evidence, sheds light on the climatic factors driving LFD occurrence and illustrates how increased occurrence and spatial extension of late-spring frosts might constrain future southern European beech forests' growth

* Corresponding author at: Universidad de Valladolid, EiFAR-iuFOR, Campus Duques de Soria s/n, 42004 Soria, Spain.
E-mail address: gabriel.sanguesa@uva.es (G. Sangüesa-Barreda).

https://doi.org/10.1016/j.scitotenv.2021.145860

and functionality. Observed alterations in the climate-phenology interactions in response to climate change represent a potential threat for temperate deciduous forests persistence in their drier/southern distribution edge.

1. Introduction

The frequency of extreme climate events, such as heat waves or extreme droughts, is increasing due to climate change (Easterling et al., 2000; Stott, 2016). Despite their long return times, extreme climate events have a disproportionate impact on forest productivity, tree demography and longevity (Allen et al., 2015; Breshears et al., 2005; Di Filippo et al., 2012; Hufkens et al., 2012), potentially constraining species range limits (Körner et al., 2016; Zimmermann et al., 2009). Understanding how recurrent extreme climate events are affecting forests is paramount to forecast forests' vulnerability to climate change.

Late frost defoliation (LFD) events are among the less studied impacts of extreme climate events on forest systems (Ummenhofer and Meehl, 2017). LFDs result from a complex interaction between two selective forces: warmer spring temperatures that promote earlier leaf unfolding, and late-spring freezing temperatures that drive plant injury (Augspurger, 2009; Inouye, 2000). In fact, temperate deciduous tree species are very sensitive to spring-frost episodes at the beginning of leaf emergence, which lead to widespread loss of leaves and flowers (Inouye, 2000). LFDs impacts are therefore not trivial, scaling from tree productivity and reproduction (Augspurger, 2011; Dittmar et al., 2006; Príncipe et al., 2017) to species distribution (Hufkens et al., 2012; Körner et al., 2016; Muffler et al., 2016). Thus, a diagnosis of temporal changes in the frequency and extension of LFDs is critical to understand the impact of climate-phenology interactions on plant performance.

The LFD risk largely depends on the interaction between species-specific freezing resistance and leaf phenology and local adaptive responses (Bigler and Bugmann, 2018). Early-leafing species rapidly maximize carbon acquisition at the expense of a greater spring-frost risk (Bigler and Bugmann, 2018). At the intraspecific level, between- and within-population variations in leaf phenology determine the LFD risk (Salmela et al., 2013). The timing of leaf unfolding has advanced in cold-limited species as a consequence of climate warming (Fu et al., 2014; Gordo and Sanz, 2009; Menzel et al., 2006). In addition, late-frost events have also advanced but at a different pace depending on the region (Scheifinger et al., 2003), modifying the period in which newly formed plant tissues are under frost risk (Augspurger, 2009, 2013). The combination of recorded and modelled temperatures has enabled to evaluate past and future frost risks, helping to decipher the link between leaf phenology and LFDs occurrence (Augspurger, 2013; Lasch-Born et al., 2018). Recently, Zohner et al. (2020) assessed plant spring-frost vulnerability at a global scale relating plant traits, leaf unfolding timing and frost resistance with climate-based proxies of LFDs. Remote sensing-based models of increasing complexity allow detecting changes in canopy reflectance associated to LFD events (Bascietto et al., 2019; Olano et al., 2021). However, studies based on in situ empirical evidence, needed to validate large-scale frost-risk models, are still scarce or limited by the temporal availability of satellite images. Due to the relatively long return times of LFD events (Olano et al., 2021), achieving multidecadal time series of frost damage records is critical to assess their long-term evolution. In this sense, the drop of annual productivity in years of LFD events is an excellent footprint to track them through the study of tree rings (Dittmar et al., 2006; Sangüesa-Barreda et al., 2019; Vitasse et al., 2019).

The analysis of predisposing climatic factors (e.g. abnormally warm springs) combined with the timing and intensity of late-spring frosts is an effective approach to determine LFDs incidence on tree growth (e.g. Vitasse et al., 2019). The growing-degree days (GDD; i.e. the accumulation of warm temperatures) are closely related to phenological responses (Clark and Thompson, 2010; Miller et al., 2000). GDD values largely exceeding the requirements for leaf unfolding indicate an unusually early onset of leaf phenology, and subsequent higher LFD risk (Vitasse et al., 2018; Vitasse et al., 2019). However, GDD requirements must be contextualized in accordance with the previous chilling (i.e. winter cold temperatures to release bud dormancy) and the day length (Fu et al., 2015, 2019), as well as the background climatic conditions (Peaucelle et al., 2019). In addition, the inclusion of other indicators more directly linked to late-frost risk, considering temperature variability during the flushing period, provides a broader context to identify damaging spring frosts.

In this paper, we assess the incidence of LFD events in European beech (*Fagus sylvatica* L., hereafter beech). Beech is one of the most widespread deciduous tree species in Europe. Its leaf phenology is driven by spring temperatures and chilling, with an interactive effect of the photoperiod (Dantec et al., 2014; Vitasse and Basler, 2013). Beech combines a recent advance of leaf unfolding of around 2.8 days per decade (Fu et al., 2015) with high sensitivity to late-frost events (Davi et al., 2011; Olano et al., 2021). Temperatures below −3 °C damage beech-young leaves (Dittmar et al., 2006), causing widespread crown defoliations and sharp secondary growth reductions (Dittmar et al., 2006; Menzel et al., 2015; Príncipe et al., 2017). We focus on the beech southern distribution limit, where water availability in summer (Piovesan et al., 2005; Rozas et al., 2015; Serra-Maluquer et al., 2019) and late-spring frosts (Gazol et al., 2019; Piovesan et al., 2003) are the main growth constraints. To buffer summer drought stress, Mediterranean beech forests are located in mountain areas where fog immersion and topographic rainfalls are frequent (Barbeta et al., 2019). Southern European beech forests have experienced marked warming trends that are forecasted to continue in the future (Giorgi and Lionello, 2008). Over the last two decades, severe LFD episodes have been reported on this species, in particular associated with abnormally warm springs (e.g. Bascietto et al., 2019; Bigler and Bugmann, 2018; Dittmar et al., 2006; Menzel et al., 2015; Príncipe et al., 2017; Vitasse and Rebetez, 2018; Vitra et al., 2017). In fact, the LFDs incidence on beech has increased 37% from 2003 to 2010 to 2011–2018 in its dry-marginal distribution limit (Olano et al., 2021). However basic questions concerning the impact of global warming trends on LFDs incidence still remain unclear. In particular, it is of interest whether a major acceleration of climate warming and shift in spring phenology is altering their frequency, and whether changes in LFDs frequency are spatially aggregated.

To answer these questions, we analyse a large dendrochronological dataset of 23 beech forests and 701 trees sampled across elevation gradients in 8 different mountain ranges in southern Europe to assess the incidence of late-spring frosts since 1950. Our specific goals are: (i) to determine which climatic parameters drive LFD incidence; (ii) to identify major LFD episodes in beech forests in the last seven decades; and (iii) to climatically and spatially characterize the reconstructed LFD events. We hypothesize that LFD events are more frequent at higher altitudes and towards beech southern distribution edge, and that the frequency of LFD events has increased in the last decades in response to recent warming trends.

2. Material and methods

2.1. Study region

The study region comprises the southern distribution edge of beech in Spain and Italy, including one site in the Austrian Alps, and covers a latitudinal range from 41° to 48° N (Fig. 1). Annual precipitation strongly varies depending on the study area, being the lowest in the southernmost Spanish beech forests (Moncayo; <800 mm), and the highest in the Italian populations (ca. from 1000 to 1200 mm; Table A1). Most precipitation falls in winter-autumn in Italian and Spanish forests, while spring and summer are the rainiest seasons in the Austrian site. Average maximum temperatures are higher towards the southernmost populations (Moncayo and Terminillo), whereas minimum temperatures are lower in Spanish than in Italian forests. Average minimum temperatures in spring range from 1.6 to 5.6 °C, being also lower in the Spanish populations. In the Austrian site, winter minimum temperatures are 2.6 to 5.6 °C lower than in the rest.

2.2. Sampling design and basal area increment chronologies

We selected eight mountain ranges: four in Spain, three in Italy and one in the Austrian Alps (Fig. 1). In each mountain range, we selected an elevational gradient and located three populations at high, middle and low elevation (except in the Autrian Alps where we only selected two populations at middle and low elevation; Table 1). In each population, we randomly selected and cored a minimum of 15 dominant or co-dominant trees. Increment cores were taken at 1.3 m height using Pressler increment borers, generally extracting two perpendicular cores of 5.15-mm diameter per tree. Samples were taken in 2017–18 in the Spanish populations, and between 2012 and 2019 in the Italian and Austrian populations. Increment cores were air-dried, mounted on standard wooden supports and progressively sanded to improve the visibility of tree-ring borders. Then, samples were visually cross-dated and measured at a minimum resolution of 0.01 mm using a VELMEX (Inc., USA) measuring system and a CTRMD (Computer Controlled Tree Ring Measure Device; Aniol, 1987) controlled by the software CATRAS (Aniol, 1983). The quality of cross-dating was evaluated using the COFECHA program (Holmes, 1983). Annual tree-ring width series were transformed to basal area increments (BAI) and averaged per tree using the *bai.out* function of the *dplR* package (Bunn et al., 2016) in R environment (R Core Team, 2018). This function calculates BAI from bark to pith considering individual trunk diameter. BAI is a more biologically meaningful variable to quantify radial growth trends and changes than tree-ring width, being less affected by tree allometry and becoming stable at tree maturity (Biondi and Qeadan, 2008). We constructed a BAI chronology per elevation and site.

2.3. Detection of potential LFD years in tree rings

We used the relative growth change method to identify potential growth reductions due to LFDs (Schweingruber et al., 1990). We defined

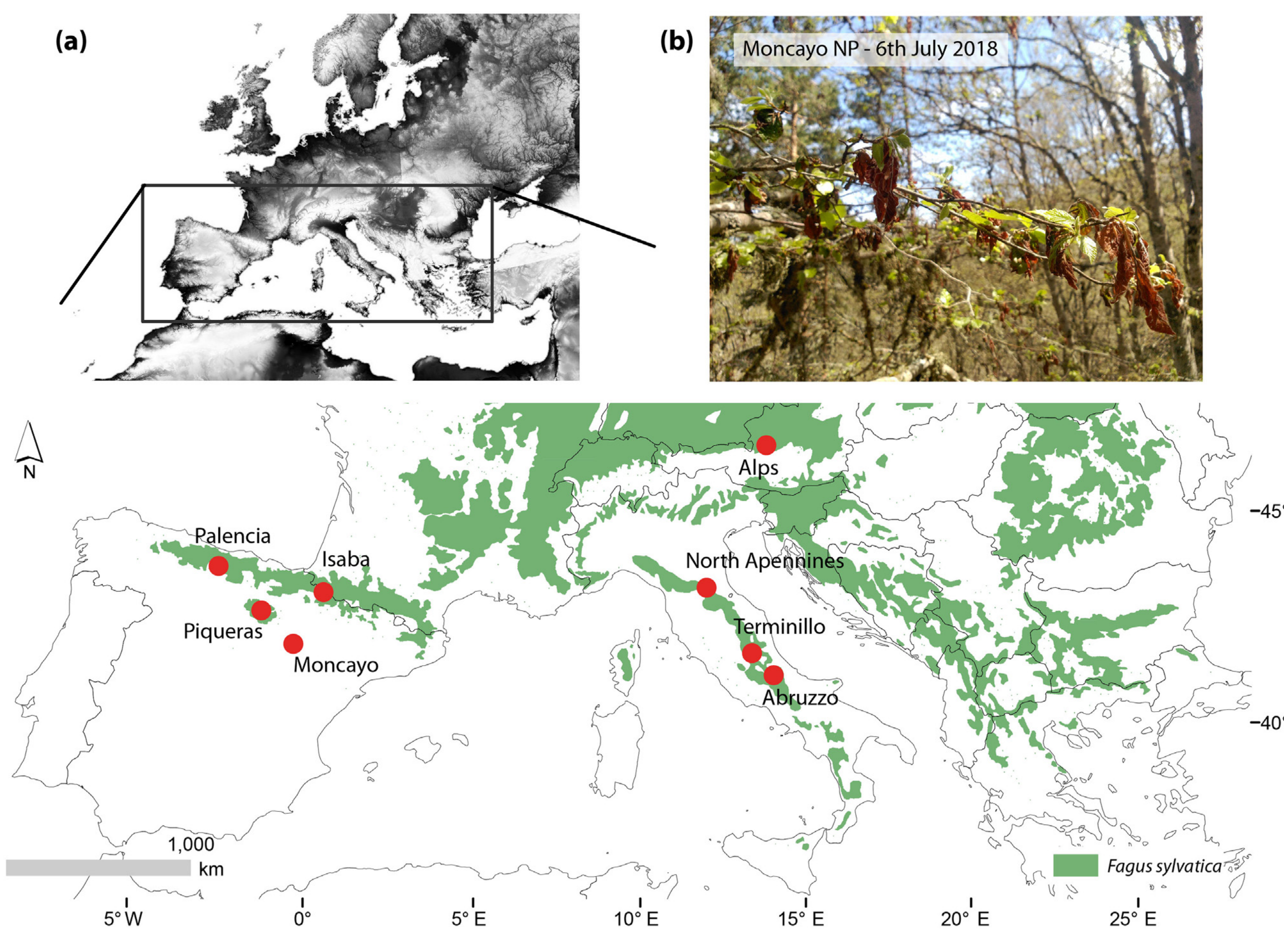

Fig. 1. a) Location of the study areas (red points). The green surface indicates the European beech (*Fagus sylvatica*) range according to the Euforgen program (http://www.euforgen.org/). The grey scale in the upper-left map represents elevation, increasing from black to white. b) A damaged beech shoot, defoliated by a late-spring frost at Moncayo forest (north-eastern Spain) in July 2018.

a negative event year as a year with at least 40% of tree-ring growth reduction with respect to the average growth in the 4 preceding years (D'Andrea et al., 2020; Príncipe et al., 2017). In this first step, we identified negative event years as candidates for LFD events. Then, we defined a pointer year when more than 50% of trees in a population showed a negative event year. We performed this analysis from 1950 to the last tree ring in each population. For this analysis, we used the *pointer.rgc* function of the *pointRes* R package (van der Maaten-Theunissen et al., 2015).

2.4. Identification of climate indicators of LFDs occurrence

We defined different climate parameters as potential indicators of spring-frost damage using daily climatic data from E-OBS v20.0e (1950–2019). This climatic repository provides homogenized and quality-controlled climatic data for all Europe (Haylock et al., 2008). We extracted daily minimum and average temperature at 0.25° (ca. 27.5 km) spatial resolution. Climate time series were directly downloaded from the Climate Explorer webpage (http://climexp.knmi.nl).

To define the set of climatic LFD indicators, we considered the timing and intensity of warm temperatures in late winter/spring as determinants of an early onset of leaf phenology, the fulfilment of chilling requirements, and the dates and intensity of late frost events. We defined the following indicators (see Fig. 2 for further illustration):

(i) Growing-degree days (GDD), defined as the sum of daily mean air temperature above 5 °C since January 1 to the DOY of the last spring frost event in that year (April–May). Accumulated winter and spring warm temperatures above a certain threshold are a good proxy for prediction leaf emergence (Vitasse et al., 2018). The more pronounced the warming before the last spring frost, the more developed the photosynthetic tissues, and the higher the risk of frost injury. Since a single grid of daily climate data covered all elevations in each sampling area, we accounted for potential differences across the elevation range by considering three different frost thresholds: the DOY of the last frost event with temperature below −4 °C (GDD_4), −2 °C (GDD_2) and 0 °C (GDD_0). We did not use a classic correction for elevation differences (−0.63 °C + 100 m a.s.l.) because the daily gridded climate data were not referred to any specific elevation. We also obtained the GDD from January 1 until a fixed date (30th April, GDD_{30Apr}) corresponding to the average date of leaf unfolding onset in beech populations of southern Europe (Guyon et al., 2011; Proietti et al., 2020).

(ii) Frost index in April (FI4), a critical month for beech phenology because of the start of leaf unfolding and the growing season (Guyon et al., 2011; Martinez del Castillo et al., 2016). An abnormally warm April followed by a late-spring frost is a characteristic climate pattern in LFD events. The frost index was obtained as:

$$FI4 = Tmean_{Apr} - Tmin_{Apr15-May15}$$

where $Tmean_{Apr}$ is the mean temperature in April and $Tmin_{Apr15\text{-}May15}$ is the absolute minimum temperature from April 15 to May 15, when late-spring frosts usually occur (Bascietto et al., 2019; Olano et al., 2021). We used a delayed time period because we considered two phenomena: warming inducing leaf unfolding, and late frost affecting unfolded leaves. High FI4 indicates a very warm April but also low minimum temperatures in the period when the photosynthetic tissues are more vulnerable.

(iii) Frost vulnerability index (FVI), considering mean temperature ten days before the late frost occurrence and defined as:

$$FVI = Tmean_{10\ days} - Tmin_{frost}$$

where $Tmean_{10\ days}$ is the mean temperature in the previous 10 days and $Tmin_{frost}$ is the absolute minimum temperature at the LFD event. To deal with elevation differences, we considered three temperature thresholds in a similar way than for GDD: the DOY with temperature below −4 °C (FVI_4), −2 °C (FVI_2) and 0 °C (FVI_0).

(iv) Last frost deviation index (LFDev) to consider the impact of the frost timing, defined as the number of days between the last frost at −4 °C ($LFDev_4$), −2 °C ($LFDev_2$) or 0 °C ($LFDev_0$) and the beginning of the frost-free period, that is, the DOY with average minimum temperatures above 0 °C (Vanoni et al., 2016; Gazol et al., 2019).

Table 1
Location and characteristics of the eight sampled mountain ranges of European beech (*Fagus sylvatica*) trees in its southernmost distribution limit in Spain, Italy and the Austrian Alps. DBH: diameter at breast height. Mean values ± standard error are shown.

Mountain range	Stand	Country	Lat (N)	Long (−W, +E)	Elevation (m a.s.l.)	DBH (cm)	Height (m)	n cores/trees	Age (yrs)	Last tree ring
Moncayo	High	Spain	41.80	−1.82	1565	36.6 ± 1.3	11.8 ± 0.7	62/25	148 ± 8	2017
	Middle		41.79	−1.80	1364	53.4 ± 2.5	19.4 ± 0.7	57/24	147 ± 7	2017
	Low		41.80	−1.81	1250	57.4 ± 3.2	19.6 ± 0.8	56/24	134 ± 24	2017
Piqueras	High	Spain	42.05	−2.77	1599	55.7 ± 1.9	17.9 ± 0.8	53/23	169 ± 12	2017
	Middle		42.07	−2.54	1428	49.1 ± 2.1	16.2 ± 0.5	40/24	117 ± 5	2017
	Low		42.06	−2.69	1261	59.8 ± 1.3	23.4 ± 0.9	57/23	197 ± 8	2017
Isaba	High	Spain	42.95	−0.79	1601	44.6 ± 1.4	13.0 ± 0.7	42/22	177 ± 12	2017
	Middle		42.94	−0.83	1399	61.9 ± 1.8	19.8 ± 0.9	31/15	280 ± 18	2017
	Low		42.93	−0.84	1072	77.5 ± 3.6	26.8 ± 0.9	30/15	170 ± 15	2017
Palencia	High	Spain	43.04	−4.47	1369	52.6 ± 3.6	15.3 ± 0.8	44/23	157 ± 11	2018
	Middle		43.05	−4.45	1211	62.9 ± 2.4	23.2 ± 0.9	46/23	133 ± 4	2018
	Low		43.05	−4.46	1045	65.5 ± 3.5	22.8 ± 1.2	43/23	173 ± 8	2018
Abruzzo	High	Italy	41.83	13.73	1780	58.9 ± 1.8	26.0 ± 1.8	96/96	295 ± 16	2017
	Middle		41.83	13.72	1503	65.7 ± 3.1	20[a]	24/24	199 ± 20	2019
	Low		41.83	13.71	1363	72.6 ± 2.6	25[a]	17/17	175 ± 25	2019
Terminillo	High	Italy	42.48	13.00	1730	53.9 ± 1.4	24.1[a]	66/66	271 ± 9	2015
	Middle		42.44	13.00	1587	43.4 ± 1.3	15[a]	21/21	83 ± 2	2013
	Low		42.53	12.94	1280	60.6 ± 1.6	20[a]	22/22	158 ± 17	2013
North Apennines	High	Italy	43.84	11.80	1450	71.3 ± 1.3	23.8 ± 5.9	83/83	242 ± 13	2017
	Middle		43.84	11.79	1150	72.8 ± 2.3	35[a]	28/28	185 ± 7	2016
	Low		43.85	11.81	674	67.7 ± 2.5	20[a]	28/28	144 ± 8	2015
Alps	Middle	Austria	47.79	14.33	1266	63.1 ± 1.6	27.2 ± 2.0	33/33	327 ± 20	2017
	Low		47.81	14.44	903	61.2 ± 2.2	20[a]	19/19	277 ± 11	2012

[a] Estimated based on the average height from the 5 tallest trees.

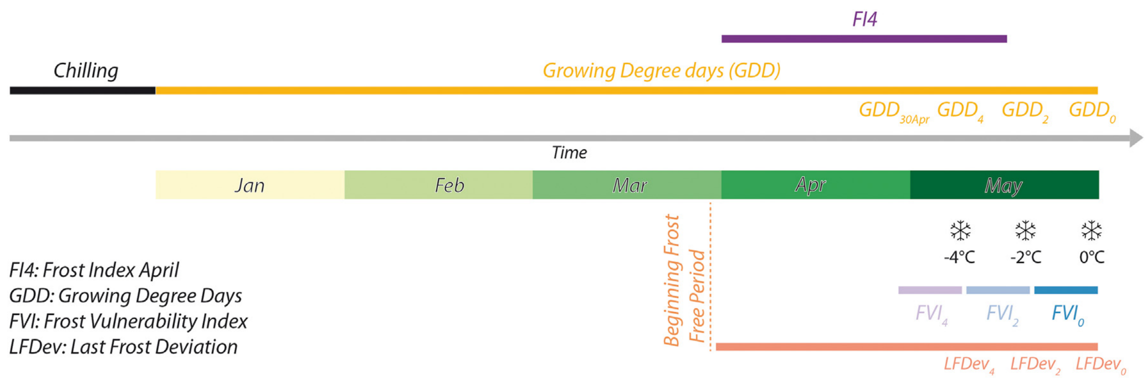

Fig. 2. Conceptual framework of the different late-frost climatic indicators used in this study. Abbreviations and definitions of late-frost indicators as in Table 2. GDD_4, GDD_2, GDD_0, FVI_4, FVI_2, FVI_0, $LFDev_4$, $LFDev_2$, $LFDev_0$ vary depending on the DOY of the last frost (−4 °C, −2 °C and 0 °C) in each year and site. The beginning of the frost-free period is the DOY with average minimum temperatures above 0 °C and varies in each site.

(v) Chilling, obtained as the number of days with a daily temperature < 5 °C from September 1st to January 1st of the calendar year preceding budburst (Dantec et al., 2014; Asse et al., 2018).

2.5. Identification of the most important LFD indicators at the population level

To determine which combinations of climatic parameters were driving LFDs incidence, we fitted linear mixed-effect models (LMMs; Pinheiro and Bates, 2000) considering annual basal area increments (BAI) as the dependent variable and the LFD indicators as fixed factors. A separate model was fitted for each population, considering the 1950–2017 period for Spanish populations and the 1950–2013 period for Italian and Austrian populations. We fitted the models at population level because leaf phenology is adapted to local climatic conditions (Peaucelle et al., 2019). We increased the analysed period in Spanish beech forests because (i) all basal area increment chronologies finished in 2017/2018 (Table 1), and (ii) to cover the major late frost event that occurred in 2017 (Olano et al., 2021).

We included tree as a random factor to incorporate the non-independent structure of our data. BAI values were log transformed prior to the analyses in order to fulfil normality assumptions, and the LFD indicators were standardized to enhance their comparability using the mean and the standard deviation of the study period. First-order autocorrelation structure (AR(1)) was also included to account for the temporal autocorrelation in BAI data. We used a multi-model inference approach based on information theory (Burnham and Anderson, 2002), fitting additive combinations of fixed factors by ranking all potential models according to the Akaike Information Criterion (AIC). To reduce collinearity between LFD indicators calculated for different frost thresholds (i.e., GDD, FVI and LFDev; Fig. 2), we only considered the frost threshold that better correlated with BAI at population level. We also considered the interaction 'GDD x chilling' as a combination of climatic variables that determines the onset of leaf phenology. Models were fitted using restricted maximum likelihood (REML), and we selected the model with the lowest AICc value and the largest Akaike weight (*Wi*). We calculated variance inflation factors (VIF) to assess collinearity among explanatory variables (Dormann et al., 2013). All models showed VIF values lower than 4 (87% of them <2.5), suggesting no longer redundancy problems among predictors (Dormann et al., 2013; Zuur et al., 2009). Residuals normality and homoscedasticity were checked to confirm the assumptions of LMMs. In the case of violations of these assumptions, models were re-fitted considering different variance covariates (Zuur et al., 2009), and we selected the model that minimized AICc. In the case of ΔAICc lower than 2, which indicates no significant differences with the second-ranked model, we opted by selecting the first one. Finally, the strength of models was evaluated by calculating the marginal (proportion of variance explained by fixed factors) and conditional (the whole model, fixed and random factors) pseudo-R^2 statistics, as proposed by Nakagawa and Schielzeth (2013). We used the R packages *nlme* (Pinheiro et al., 2014) to fit LMMs, *MuMIn* (Barton, 2012) to perform the multi-model selection and to calculate pseudo-R^2, and *performance* (Lüdecke et al., 2020) to calculate VIF and assess multicollinearity. In addition to LMMs, non-parametric Spearman correlations were calculated between BAI chronologies (at the population level) and LFD indicators. Finally, temporal trends of LFD indicators were assessed by computing the Kendall's tau statistics in the study period.

2.6. Identification of LFD events and validation from satellite data

At the population level, we considered an LFD event when a pointer year (i.e. a significant growth reduction based on tree-ring width patterns) was concurrent with values >1.5 standard deviation (upper Q3 or outliers) of one or several of the selected LFD indicators in the corresponding LMMs. We used two independent sources of validation for 21st century events. In Spain, LFD events since 2003 were validated by analyzing Normalized Difference Vegetation Index (NDVI) time series (from March to July) with an 8 days frequency using MODIS Vegetation Index Products MOD13Q1 and MYD13Q1 (Olano et al., 2021). We used a semi-supervised machine learning model to classify late frost and non-late frost pixels. For this task, we used a binary classifier called Support Vector Machine with Global Alignment Kernel. We first trained the model using a small dataset consisting of annotated pixels where LFD events were or were not recorded in 2017. Once this model was trained, it was used to predict frost damage in other geographical areas and years. Finally, we validated the model using Sentinel 2 and Landsat images from the Google Earth Engine platform (see further details in Olano et al., 2021). In some study sites, values of the LFD indicators for 2010 and 2013 episodes were in the Q3 but below the 1.5 SD threshold. However, since both events were confirmed through remote sensing data, they were considered as actual LFD events. In Italy, LFD events since 2000 were validated by comparing the May–June Enhanced Vegetation Index (EVI) of these years with the 2000–2018 median. For each forest, we used MOD13Q1 data at 250 m-pixels resolution, considering those pixels whose centroid was closer than 500 m to the centroid of the dendroecological sampling (Di Fiore et al., submitted). Both NDVI and EVI time series have a significant correlation with phenological ground observations, particularly for deciduous broadleaf forests (Peng et al., 2017; Testa et al., 2018).

2.7. Climatic characterization and spatial incidence of LFDs

To establish regional climatic similarities in the identified LFD events, we used Principal Component Analyses (PCAs) based on the variance-covariance matrix including all late-frost indicators after standardization (Fig. 2). We performed a single PCA per study area using the *FactoMineR* R package (Lê et al., 2008), and the results were visualized using the *Factoextra* R package (Kassambara and Mundt, 2016). Finally, we evaluated the spatial extent of the last LFD events using the ESRL website (https://www.esrl.noaa.gov/psd/cgi-bin/data/composites/plot20thc.day.v2.pl) to plot daily composites of the mean temperature. We considered three different atmosphere elevations at 800, 850 and 900 mb, which correspond to around 2000, 1500 and 1000 m a.s.l., respectively. We considered the DOY of the LFD event as the DOY of the last spring freezing event in that year.

3. Results

3.1. Growth patterns and dendrometric characteristics of studied beech trees

The mean growth rate in the study period decreased from the low-elevation populations to the high-elevation sites (Fig. A1). At study area level, the lowest mean growth rates were found in Moncayo (1.14 mm) and the highest in North Apennines (1.71 mm). Mean age of sampled trees was 189 years (min. 83 and max. 327 years), reaching the maximum age in the middle-elevation Austrian Alps population (Table 1). Mean trunk diameter was 53.5 cm (36.6–77.5 cm) and showed a negative trend with elevation. Mean height was 21.1 m (11.8–35 m), with taller trees growing at the low elevation sites.

3.2. LFD indicators related to beech tree growth

Selected LMMs accounted for 21–77% of the total BAI variance, 1–12% of which was uniquely explained by LFD climate indicators (Table 2). Climatic factors promoting LFD events had higher explanatory power at high altitude, thus indicating a greater relevance of LFDs on growth, particularly in Spanish and the southernmost Italian population (Abruzzo). By contrast, LFD indicators had low or very low explanatory power in the northern Italian populations (North Apennines) and the Austrian Alps.

GDD had a negative effect on BAI in 14 out of 23 populations, particularly in high-elevation Spanish populations and at the southernmost Italian area (Table 2, Fig. A2 and Table A2). By contrast, GDD favoured growth in those sites where LFD indicators had low or very low explanatory power (North Apennines and Austrian Alps; Table A2). The interaction between GDD and chilling was important in the western Spanish populations (Piqueras and Palencia), increasing its relevance with elevation (Table 2). In 14 out of 23 populations, chilling showed a negative effect on growth. FI4 was negatively and significantly related to BAI in 10 out of 23 populations, as FVI was in 7 out of 23 sites, especially FVI_0. Lastly, the last frost timing (LFDev) negatively influenced growth in 15 out of 23 populations, with $LFDev_0$ being better indicator than $LFDev_4$.

The temporal trends of LFD indicators were divergent. GDD_{30Apr} values increased in all studied populations since 1950 as a consequence of warmer conditions (Table A3), whereas LFDev showed a negative trend, mainly in Spain (Moncayo and Isaba) and the Austrian Alps. Finally, FI4 and FVI did not show significant temporal trends.

3.3. Reconstruction of major LFD events since 1950

The concordance between extreme values of significant climatic LFD indicators and sharp reductions in annual radial growth supports the occurrence of LFD episodes since 1950 (Figs. 3 and 4). LFD events were relatively rare considering that the shortest return time was 13.4 years (Moncayo; Fig. 5). However, the frequency of LFD events increased since the 1990s, in particular in Spanish beech forests and at the southernmost Italian populations (Abruzzo; Fig. 5). The average return time changed from 33.1 years (with a minimum of 19.5 and a maximum of 39 years) before 1990 to 14.1 years since then (6.75 years in Moncayo – 23 years in North Apennines and Alps; Fig. 5). The last LFD events (2010, 2013 and 2017 in the Spanish populations, 2013 and 2016 in Abruzzo and Terminillo) were validated through the assessment of satellite-derived indices of vegetation activity (Figs. A3, A4 and A5). In some study sites, LFD events of 2010 and 2013 could be identified by other means, even if they did not show values above the 1.5 SD threshold (standardized values >1.5; Fig. 4). However, the increased LFDs temporal trend was maintained even after excluding these two events (Table A4). The last episodes (1997, 1999, 2010, 2013 and 2017) were largely coincident in all sampled Spanish populations, suggesting that the area damaged by LFD events has increased over time (Fig. 3). The late-spring frost event of 2013 was also evident in all studied Italian beech areas. In contrast, before the 1990s, LFD events were geographically isolated, just affecting one or two study areas.

3.4. Climatic and geographic characterizations of LFD events

Climatic characteristics of reconstructed LFD events differed among years and study areas. In the Spanish beech populations, 1997 and 2017 LFD events showed warm temperatures in spring (high GDD and FI4 values; Figs. 4 and A6). Similarly, LFD events in 1999 and 1977 in Moncayo showed high GDD_4 and FI4 values, in line with the date of the damaging frost occurred by late April (Fig. A7). Contrarily, LFD events in 2010 and 2013 were associated with moderately warm temperatures in April (FI4) and with very late spring frosts (Figs. 4, A6 and A7). In the Italian populations, LFD events in 1998 and 2016 in Abruzzo corresponded to very warm spring temperatures (GDD_{30Apr}). The 1962 event was there associated with warm temperatures during shorter time windows (FVI_0), and the 1957 event, with a very late spring frost. LFD events in Terminillo (1962 and 1981) and North Apennines (1981) were also related to high FI4 and FVI values. In the three Italian study areas, the LFD event of 2013 was related to high GDD_{30apr} and FVI values. Finally, in the Austrian Alps, the 2011 event showed high FI4 values, while 1977 and 1986 events were associated with high values of GDD_4, $LFDev_4$ and FI4 (Figs. 4 and A6).

The frost event in late May 2013 caused LFDs in beech forests coinciding with generalized temperatures below 0 °C above 1500 m a.s.l. (Fig. A7). Although the 2010 LFD event was less extensive, it affected all northern Spain, which is in line with the growth reductions observed in our tree-ring series (Fig. 3). On the other hand, the frost events in late April 1999 and early May 1997 affected different northern Spanish populations depending on the leaf unfolding dates (Fig. 3 and A7).

4. Discussion

Our study shows that the frequency of late-frost damage has increased in the beech southern distribution edge since the 1990s due to progressive spring warming and associated shifts in leaf phenology (Bigler and Bugmann, 2018; Fig. 5). The average return time changed from 33.1 years before 1990 to 14.1 years after 1990 (Fig. 5). However, this trend showed a strong geographic pattern. LFD events frequency did not increase at higher-latitude mountain ranges, i.e. North Apennines and Austrian Alps. In contrast, the Spanish and southernmost Italian beech forests showed a sharp increase in late-frost risk (Fig. 5). In general, radial growth of beech was more limited by LFD events at higher altitude (Table 2), as previously stated by several authors (Dittmar et al., 2006; Olano et al., 2021; Zohner et al., 2020). Finally, recent LFD events seem to be impacting larger geographical areas than previous episodes, as the 2013 event was observed across the entire southwestern beech distribution range in Spain and Italy. Our study sheds light on the climatic factors driving LFDs occurrence by

Table 2
Statistics (t-value) of the selected linear-mixed effects models fitted to the basal area increment (BAI; log transformed) in each area and elevation as a function of different late-frosts indicators (see more details below) for the 1950–2017 period in Spanish populations and for the 1950–2013 period in Italian and Austrian populations. The model showing the lowest Akaike Information Criteria (AICc) was selected as the best model. The ΔAICc shows the difference in AICc between the first and second-ranked model, the Akaike weight (Wi) is the probability that the selected model is the best one, and DF are degrees of freedom. Values in the last column indicate the marginal (fixed factors alone) and conditional (fixed and random factors; between parentheses) pseudo-R^2 values, respectively.

Area (country)	Elevation	GDD				chilling	GDD ∗ chilling	FI4	FVI		LFDev		DF	Wi	ΔAICc	R^2
		GDD_4	GDD_2	GDD_0	GDD_{30Apr}				FVI_4	FVI_0	$LFDev_4$	$LFDev_0$				
Moncayo (SP)	High				−5.00**	3.41**		−6.08**				−12.67**	1660	0.46	0.03	0.05(0.41)
	Middle							−7.25**				−10.19**	1602	0.82	3.25	0.01(0.77)
	Low	−7.96**				−3.94**						−15.97**	1605	0.63	3.03	0.03(0.29)
Piqueras (SP)	High			−18.87**		1.27	12.81**						1532	0.94	6.72	0.12(0.32)
	Middle			−5.05**		−1.65*	8.43**					−4.55*	1598	0.97	7.16	0.04(0.36)
	Low			−0.52		−1.99*	8.39**	−5.43**				−9.20**	1599	0.99	10.82	0.05(0.43)
Isaba (SP)	High		−5.35**			1.45	8.17**			−8.36**		−6.48**	1469	0.52	0.22	0.09(0.52)
	Middle		−10.72**			3.55**		3.75**				−9.33**	1068	0.53	2.30	0.11(0.41)
	Low					−4.00**			−4.42**			−4.78**	1001	0.86	4.97	0.03(0.30)
Palencia (SP)	High			−7.95**		−1.48	8.43**	−2.97*					1537	0.62	1.92	0.05(0.40)
	Middle			1.59		−2.08*	6.91**	−5.71**				−8.53**	1518	0.98	8.19	0.03(0.51)
	Low			2.74*		−1.23	6.16**	−5.50**				−7.71**	1536	0.43	0.68	0.03(0.49)
Abruzzo (IT)	High				−17.86**	−12.85**				−12.64**	−5.86**		5424	0.71	6.69	0.05(0.64)
	Middle				−8.41**	−6.16**				−5.66**		−4.74**	1237	0.70	2.04	0.06(0.49)
	Low				−3.83**	−3.54**				−7.35**			954	0.34	1.57	0.05(0.21)
Terminillo (IT)	High				−17.11**	−6.60**				−5.65**			3824	0.29	0.10	0.03(0.57)
	Middle				−3.64**			−5.29**					1284	0.70	1.79	0.01(0.35)
	Low				−5.19**			−3.81**					1290	0.74	2.37	0.01(0.43)
North Apennines (IT)	High					−7.89**		−10.64**		−5.97**		7.43**	5194	0.98	8.98	0.01(0.43)
	Middle	4.21**				−2.63*	4.73**				−5.46**		1728	0.96	6.99	0.01(0.46)
	Low												–	–	–	–
Alps (AU)	Middle	5.34**				−3.36**	7.10**	−8.31**			−4.56**		1959	0.98	10.13	0.02(0.28)
	Low											−5.49**	1147	0.75	3.58	0.01(0.46)

Abbreviations (see Fig. 2): *GDD:* Growing Degree Days since January 1 to the DOY of the last frost (0 °C –GDD_0–; −2 °C –GDD_2-; −4 °C –GDD_4-,), or to 30th April (GDD_{30Apr}). *chilling*: number of days with a daily temperature < 5 °C from September 1 to January 1 of the calendar year preceding the growing season. *FI4*: April Frost Index, obtained as the mean temperature in April minus the absolute minimum temperature between April 15 and May 15. *FVI:* Frost Vulnerability Index, obtained as the mean temperature in the previous 10 days at the DOY of the last frost (0 °C –FVI_0–; -4 °C –FVI_4–) minus the absolute minimum temperature. *LFDev:* Last Frost Deviation, obtained as the number of days between the last frost (0 °C –$LFDev_0$–; -4 °C –$FFDev_4$–) and the beginning of the frost-free period (DOY with average minimum temperature above zero degrees). Note: In North Apennines-Low no model significantly explained growth.

* $P < 0.05$ significance level.

** $P < 0.001$ significance level.

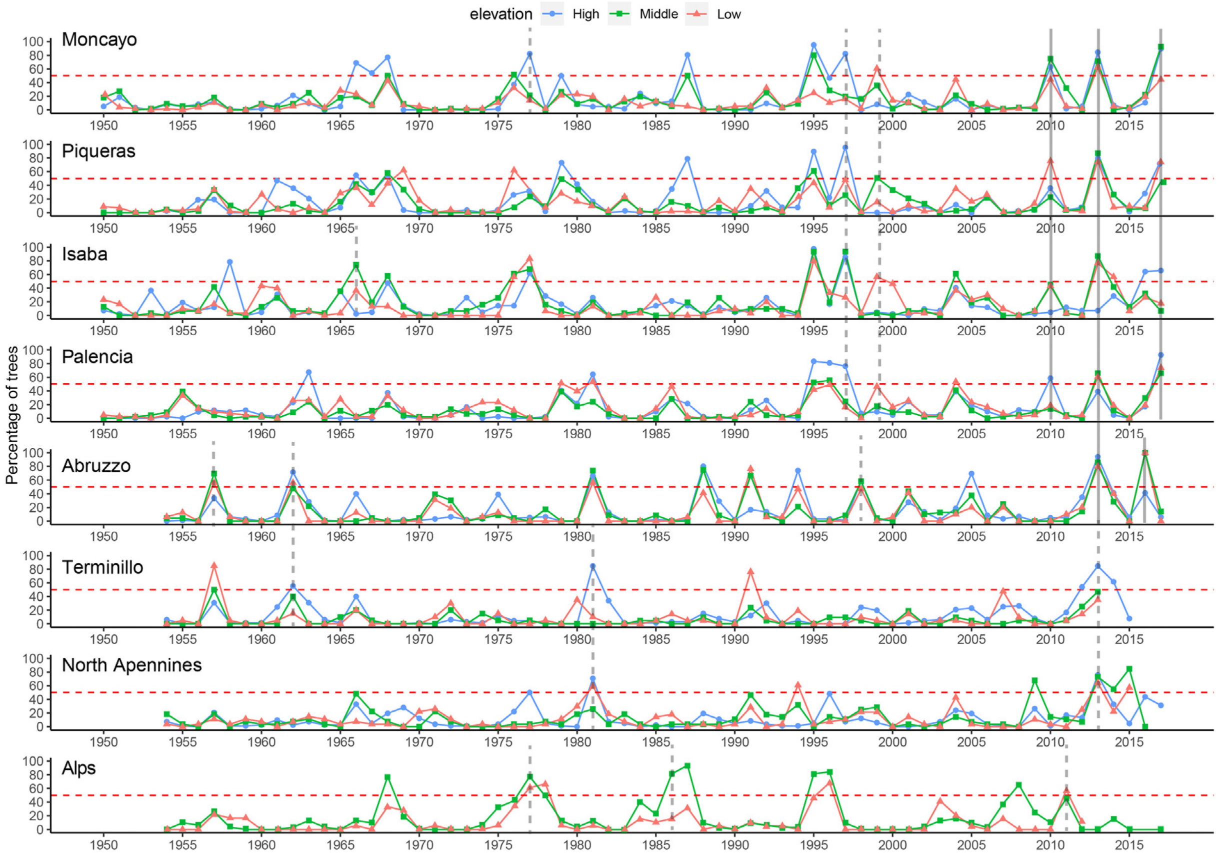

Fig. 3. Percentage of trees that showed negative event years at each location and elevation, based on tree-ring width patterns. We considered a pointer year when at least 50% of the trees showed a negative event year (i.e., over the horizontal dashed red line). Vertical solid grey lines indicate LFD events detected by climate indicators, tree ring and remote sensing data. Vertical dashed lines correspond to LFD events detected by climate indicators and tree ring data.

considering the scale of spring warm temperatures, and the timing and intensity of late-spring frosts.

The suitability of our approach was validated through remote sensing data in the last LFD events. Some of the identified LFD events had been previously cited, such as 1957 (Piovesan, 1998; Vitasse et al., 2019), 1981 (Vitasse et al., 2019), 2011 (Menzel et al., 2015; Muffler et al., 2016), and 2016 (Bascietto et al., 2019). Other stressors and processes, such as drought or masting, may induce sharp radial growth reductions and could be confounded with LFD events. The impact of these phenomena shows different patterns that enable LFD identification without assessing these events directly from climatic data. Drought stress induces growth reduction in beech forests, but its impacts are more important at low elevations, whereas LFDs incidence showed just the opposite trend (Table 2; Fig. 5). Beech masting also results in lower rates of wood production due to a trade-off between massive seed production and radial growth (Piovesan and Adams, 2002). However, the occurrence of freezing temperatures in April/May, which also damage flowers, limits the misidentification of mast years as LFD events.

4.1. Warm temperatures in spring and last frost timing drive frost damage in beech

Warmer temperatures in spring promote an earlier leaf and wood phenology, leading to higher photosynthetic gains and growth rates (Di Filippo et al., 2007; Martinez del Castillo et al., 2016; Rozas et al., 2015). However, our findings showed the opposite result; the accumulation of warm temperatures in late winter and spring (GDD) was associated with lower growth rates (Table 2). Since water is not a limiting factor in early spring, this association would suggest that the greater increase in late-frost risk combined with an earlier leaf flush outpace the benefits of a longer growing season. Nevertheless, this result was spatially heterogeneous. The low-elevation forests in the North Apennines and Austrian Alps showed positive GDD-growth associations (Table A2), supporting a lower LFDs incidence (Tables 2 and 3). The positive relationship between GDD and late-frost damage was reinforced when other indicators directly linked to late-frost risk at the middle and short term (FI4 and FVI) were considered. Warm temperatures in April accelerate leaf sprouting, leaving large beech areas exposed to damaging freezing temperatures. The timing of the last frosts was also relevant, since later frosts exerted greater impacts as indicated by the negative LFDev-growth associations (Table 2). In addition, frost intensity also modulates the defoliation degree, potentially damaging the meristems in the most severe cases.

Interpreting the effect of chilling is more complex. Chilling may be an indicator of cold winter having a negative impact on growth through cold damage by frost-induced xylem embolism (Muffler et al., 2020; Weigel et al., 2018). In fact, the negative effect of chilling increased upwards, where extreme low winter temperatures are frequent. Otherwise, the interaction of chilling with GDD was only relevant for growth of western Spanish populations. Nevertheless, this result should be interpreted with caution because the goal of this study is not to evaluate the role of chilling temperature on leaf unfolding dates, but rather to consider the potential interaction of chilling and GDD as a determinant of a very early onset of leaf phenology and thus high LFD risk. In this sense, clarifying the mechanisms of this positive interaction on growth requires further research.

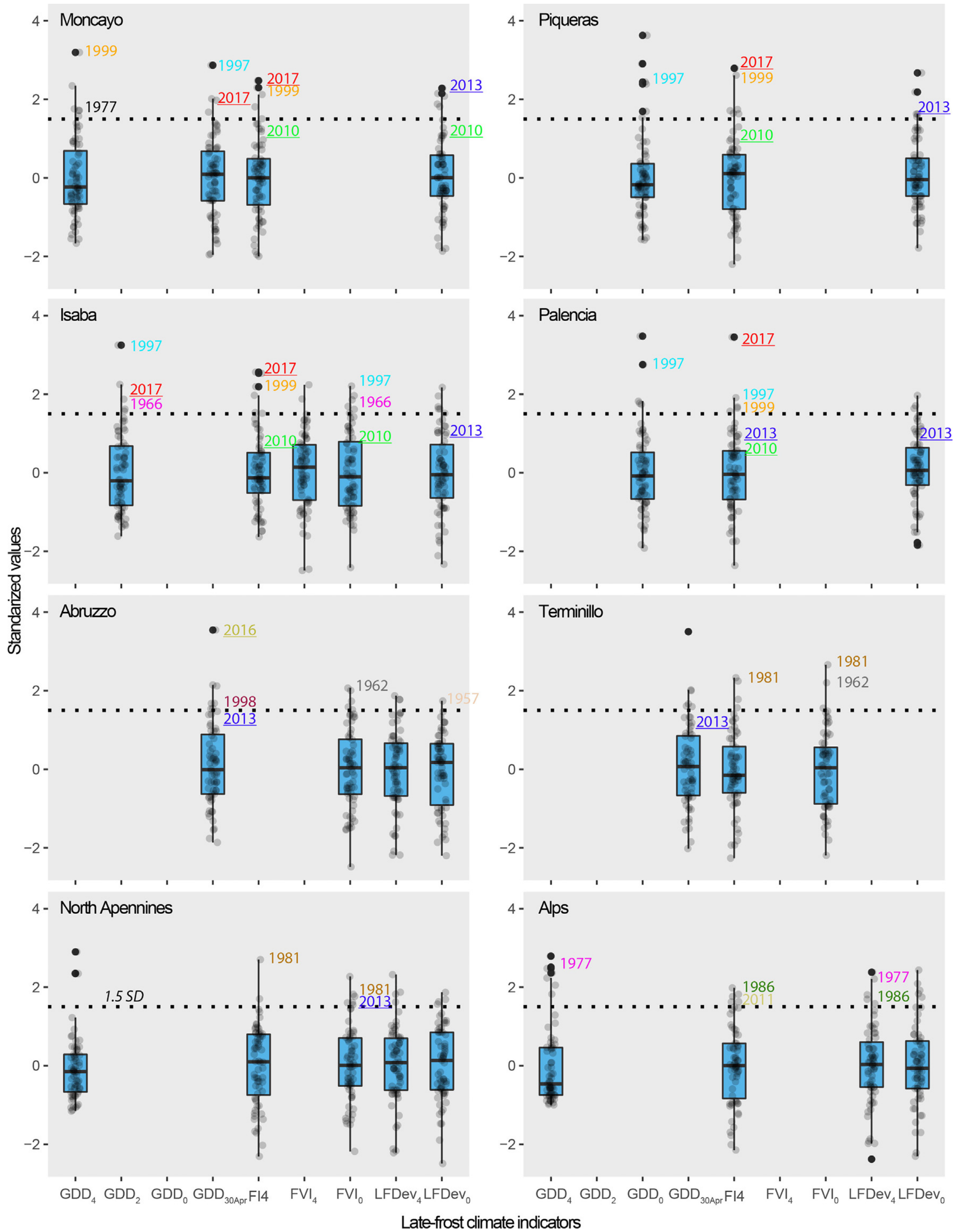

Fig. 4. Boxplots of yearly values (grey points; outliers as black points) of the late-frost climate indicators selected in the Linear Mixed-Effect models (see Figs. 2 and Table 2) for each study area. The years identified as LFD events in Fig. 3 are highlighted. Same LFD events are represented with the same colour in all panels. Underlined LFD events were validated through remote sensing data. Dashed horizontal lines represent the 1.5 SD threshold.

Warm temperatures at long- and middle-term (GDD and FI4) were the best LFD indicators, in particular for populations at high elevation (Table 2). There was great variability depending on the region, which suggests potential local adaptations to local climatic envelopes (Peaucelle et al., 2019). The last frost timing (LFDev) was also relevant in most sites, especially in the Spanish populations, highlighting the high vulnerability when the beginning of beech leaf emergence simultaneously occurs over large areas.

4.2. Late-frost damage has increased at the southernmost beech forests

Warmer springs have favoured an earlier onset of leaf unfolding along beech distribution area (Bigler and Bugmann, 2018; Fu et al., 2015; Menzel et al., 2006). In southern European beech forests, late-winter and spring temperatures have increased faster than the advance in the date of the last-spring frost (Table A3), thus likely lengthening the late-frost risk window. This trend is compatible with the increased a)

Area (country)	Elevation	N LFD (return time) Total	1950-1989	1990-last ring	
Moncayo (SP)	High	5 (13.4)	1 (39.0)	4 (6.7)	+
	Middle	3 (22.3)	0	3 (9.0)	+
	Low	2 (33.5)	0	2 (13.5)	+
Piqueras (SP)	High	3 (22.3)	0	3 (9.0)	+
	Middle	2 (33.5)	0	2 (13.5)	+
	Low	3 (22.3)	0	3 (9.0)	+
Isaba (SP)	High	2 (33.5)	0	2 (13.5)	+
	Middle	3 (22.3)	1 (39.0)	2 (13.5)	+
	Low	2 (33.5)	0	2 (13.5)	+
Palencia (SP)	High	3 (22.3)	0	3 (9.0)	+
	Middle	2 (33.5)	0	2 (13.5)	+
	Low	2 (33.5)	0	2 (13.5)	+
Abruzzo (IT)	High	3 (21.0)	1 (39.0)	2 (11.5)	+
	Middle	4 (15.8)	1 (39.0)	3 (7.7)	+
	Low	4 (15.8)	2 (19.5)	2 (11.5)	
Terminillo (IT)	High	3 (21.0)	2 (19.5)	1 (23.0)	-
	Middle	0	0	0	
	Low	0	0	0	
North Apennines (IT)	High	2 (31.5)	1 (39.0)	1 (23.0)	
	Middle	1 (63.0)	0	1 (23.0)	+
	Low	2 (31.5)	1 (39.0)	1 (23.0)	
Alps (AU)	Middle	2 (31.5)	2 (19.5)	0	-
	Low	2 (31.5)	1 (39.0)	1 (23.0)	

+ Increasing late frost defoliations
No evident changes
- Decreasing late frost defoliations

b)

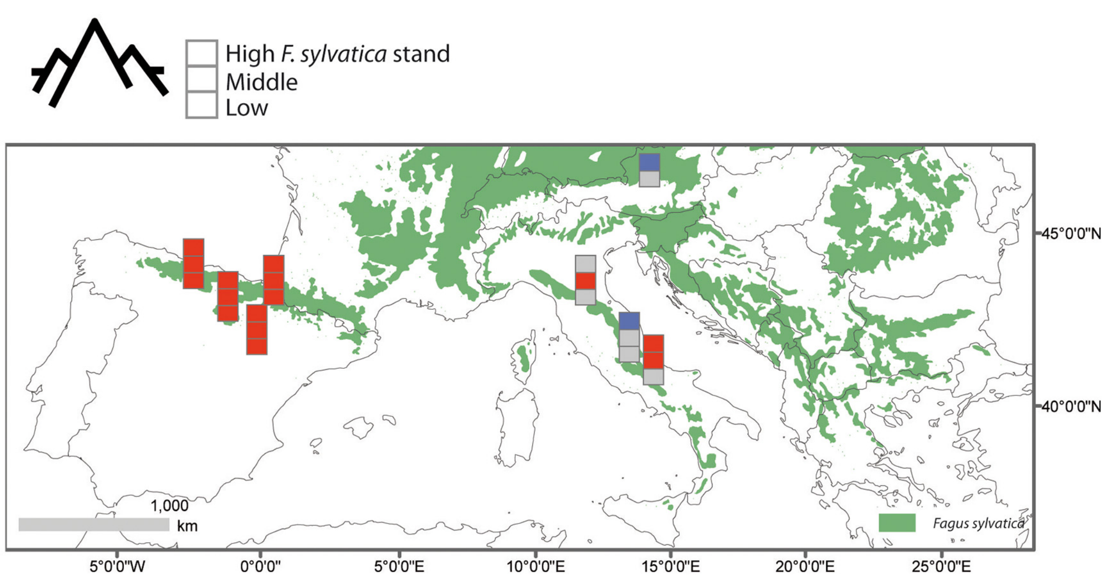

Fig. 5. a) Number of LFD events in the whole study period (1950–2013 for Italian and Austrian beech populations, 1950–2017 for Spanish beech populations) and before and after 1990. The values in brackets indicate the return time (years) in each population and period. The last right column shows the trend in LFDs frequency (positive –red-, negative –blue-, or no changes –grey-). b) Geographical structure of the changes in LFDs frequency.

frequency of LFD events observed in our study, which is in line with the latest major LFD events that consecutively damaged Italian and Spanish beech forests in the last years (Bascietto et al., 2019; Olano et al., 2021).

Detecting changes in LFD risk in forests is emerging as a high-priority topic. Current knowledge suggests that LFD trends show strong regional variation. Increases in LFDs frequency have been found for Finland (Hänninen, 1991), eastern North America (Augspurger, 2013), and areas of Europe and Asia (Zohner et al., 2020), but no changes have been detected in central Europe (Kramer, 1994; Scheifinger et al., 2003; Lasch-Born et al., 2018). Such regional differences are consistent with the absence of changes in late-frost risk observed in the North Apennines and the Austrian Alps. These disparate results may respond to spatially heterogeneous phenological responses to climate warming, with populations and/or species exhibiting higher temperature requirements to delay leaf unfolding and to prevent late frosts (Peaucelle et al., 2019). In this sense, southern beech populations, limited by water shortage in summer, might have extended the growing season further than northern populations, increasing their susceptibility to late-frost occurrence. Finally, higher cold acclimation might translate into higher frost resistance in spring (Kalberer et al., 2006).

Late-spring frost risk increased with elevation (Dittmar et al., 2006; Olano et al., 2021; Zohner et al., 2020). Southern beech populations inhabit mountain ranges to mitigate summer drought stress, and elevation increases the frequency of damaging freezing temperatures in late spring (Bigler and Bugmann, 2018). Moreover, the advance in phenology is faster at high elevation (Vitasse et al., 2018) due to the combination of more intense warming trends (Pepin et al., 2015) and less limiting photoperiod and chilling. In fact, the safety margins, i.e. the difference between the onset of leaf unfolding and the last spring frosts, are narrower in forests located at high elevation than at lowlands (Bigler and Bugmann, 2018; Vitasse et al., 2018). In agreement with the latter explanation, high-elevation beech trees take advantage of cold conditions in April and warmth in May, which are linked to the need of escaping late frosts during the first phases of the growing season (Di Filippo et al., 2007; Piovesan et al., 2005). This result has also been observed in core populations, where the signal of low temperatures in April has become significant in the last decades (Muffler et al., 2020).

Most of the LFD events were associated with extraordinarily warm springs (Fig. 4). The coupling of leaf unfolding with lethal late-spring frosts determined the spatial extension of damage across the elevation range. For instance, the frost event in late April 1999 only affected low- and middle-elevation populations because high-elevation sites had not yet flushed (Fig. 3 and A7). By contrast, the frost event in May 1997 mostly affected high- and middle-elevation sites because leaf unfolding was coincident with the frost, whereas in low-elevation populations the low temperatures were probably not cold enough to cause damage, and more mature leaves are more freezing resistant (Vitra et al., 2017).

4.3. Southern beech populations in a context of warmer and drier climate conditions

Secondary growth of southern beech populations is sensitive to late spring-summer water shortage (Di Filippo et al., 2007; Jump et al., 2006; Piovesan et al., 2005; Rozas et al., 2015), but late-spring frosts may also play a relevant role (Gazol et al., 2019). The southwestern beech populations have shown a growth decline after the climate shift occurred in the 1980s (Serra-Maluquer et al., 2019), which could be a response to the combination of increasing drought stress and LFDs occurrence. Southern beech populations are prone to experience a combination of different negative impacts occurring in the same growing season, which means LFD in late spring and water shortage in late spring/summer. Indeed, the combined effect of both stressors could promote non-linear responses (Buma, 2015), even if modeling approaches do not report larger growth impacts (Gazol et al., 2019).

Global warming is threatening southern beech populations by increasing drought intensity and aridity (IPCC, 2014). Despite some populations seem to be adapted to water shortage (Muffler et al., 2020), increasing drought stress could promote an upward migration (Jump et al., 2006; Peñuelas and Boada, 2003). However, moving towards higher elevations might not be a successful solution. First, a greater frost incidence concentrated at higher elevation could limit the ability of southern beech populations to cope with drought. Second, the selective LFDs incidence on deciduous species could reduce their competitive ability in mixed forests (Hufkens et al., 2012), as has been observed with the unexpected spreading of *Pinus heldreichii* in old-growth high-elevation beech forests (Piovesan, 2019). Third, LFDs impacts may go beyond reductions in radial growth and include, for instance, major impacts on reproduction (Inouye, 2000). Thus, higher frost incidence at higher elevation could also imply changes in forest composition and dynamics and in the associated flora and fauna (Bogdziewicz et al., 2020).

5. Conclusions

Beech populations inhabit mountain ranges along its southern distribution range to mitigate summer-drought stress. Their higher elevation with respect to populations at the core of their distribution may suppose a higher vulnerability to LFDs for southern populations. Our results, based on climate data and tree-ring records, confirm that LFD events are increasing in frequency and extension since 1990. This situation can be interpreted as a change in the climate-phenology interactions in response to climate change. Considering the wide study area, beech genetic differences among regions (Chmura and Rozkowski, 2002; Stojnic et al., 2013) might also explain variations in LFD incidence. The increasing incidence of LFDs and the projected water deficit for the next decades require new studies to shed light on the future implications of a combined effect of both stressors. Establishing the temporal context of this phenomenon through the evaluation of late-frost incidence beyond instrumental periods remains a challenge for future researches. In this sense, anomalies in tree-ring anatomical traits or in intra-annual wood density may help to identify LFD rings.

CRediT authorship contribution statement

Gabriel Sangüesa-Barreda: Conceptualization, Methodology, Software, Formal analysis, Investigation, Data curation, Writing – original draft, Writing – review & editing, Visualization. **Alfredo Di Filippo:** Conceptualization, Data curation, Supervision, Writing – review & editing. **Gianluca Piovesan:** Conceptualization, Data curation, Supervision, Writing – review & editing. **Vicente Rozas:** Conceptualization, Data curation, Writing – review & editing, Funding acquisition. **Luca Di Fiore:** Data curation, Writing – review & editing. **Miguel García-Hidalgo:** Data curation, Writing – review & editing. **Ana I. García-Cervigón:** Conceptualization, Data curation, Writing – review & editing. **Diego Muñoz-Garachana:** Data curation. **Michele Baliva:** Data curation. **José M. Olano:** Conceptualization, Data curation, Supervision, Writing – original draft, Writing – review & editing, Funding acquisition.

Declaration of competing interest

The authors declare no conflict of interests.

Acknowledgements

This research was funded by projects spRING (CGL2017-87309-P; Ministerio de Ciencia e Innovación, Gobierno de España) and SEÑALES (VA026P17; Junta de Castilla y León and UE-FEDER). GS-B was supported by two Spanish Ministry of Economy, Industry and Competitiveness Postdoctoral grants (FJCI 2016-30121 and IJC2019-040571-I; FEDER funds). AIG-C was supported by the Spanish MINECO (Juan de la Cierva-Incorporación grant IJCI-2017-34052) and Comunidad de

Madrid (project REMEDINAL TE-CM S2018/EMT-4338). MG-H was supported by an FPI contract (PRE2018-084106) from Spanish MICINN. The editor and three referees contributed to improve the manuscript.

Appendix A. Supplementary data

Supplementary data to this article can be found online at https://doi.org/10.1016/j.scitotenv.2021.145860.

References

Allen, C.D., Breshears, D.D., McDowell, N.G., 2015. On underestimation of global vulnerability to tree mortality and forest die-off from hotter drought in the Anthropocene. Ecosphere 6, 1–55. https://doi.org/10.1890/ES15-00203.1.

Aniol, R.W., 1983. Tree-ring analysis using CATRAS. Dendrochronologia 1, 45–53.

Aniol, R.W., 1987. A new device for computer assisted measurement of tree-ring widths. Dendrochronologia 4, 135–141.

Asse, D., Chuine, I., Vitasse, Y., Yoccoz, N.G., Delpierre, N., Badeau, V., Delestrade, A., Randin, D.F., 2018. Warmer winters reduce the advance of tree spring phenology induced by warmer springs in the Alps. Agric. For. Meteorol. 252, 220–230. https://doi.org/10.1016/j.agrformet.2018.01.030.

Augspurger, C.K., 2009. Spring 2007 warmth and frost: phenology, damage and refoliation in a temperate deciduous forest. Funct. Ecol. 23, 1031–1039. https://doi.org/10.1111/j.1365-2435.2009.01587.x.

Augspurger, C.K., 2011. Frost damage and cascading negative effects on *Aesculus glabra*. Plant Ecol. 212, 1193–1203. https://doi.org/10.1007/s11258-011-9897-z.

Augspurger, C.K., 2013. Reconstructing patterns of temperature, phenology, and frost damage over 124 years: spring damage risk is increasing. Ecology 94, 41–50. https://doi.org/10.1890/12-0200.1.

Barbeta, A., Camarero, J.J., Sangüesa-Barreda, G., Muffler, L., Peñuelas, J., 2019. Contrasting effects of fog frequency on the radial growth of two tree species in a Mediterranean-temperate ecotone. Agric. For. Meteorol. 264, 297–308. https://doi.org/10.1016/j.agrformet.2018.10.020.

Barton, K., 2012. MuMIn: multi-model inference. R package version. 1.7, p. 7 Retrieved from. http://CRAN.R-project.org/package=MuMIn.

Bascietto, M., Bajocco, S., Ferrara, C., Alivernini, A., Santangelo, E., 2019. Estimating late spring frost-induced growth anomalies in European beech forests in Italy. Int. J. Biometeorol. 63, 1039–1049. https://doi.org/10.1007/s00484-019-01718-w.

Bigler, C., Bugmann, H., 2018. Climate-induced shifts in leaf unfolding and frost risk of European trees and shrubs. Sci. Rep-UK 8, 9865. https://doi.org/10.1038/s41598-018-27893-1.

Biondi, F., Qeadan, F., 2008. A theory-driven approach to tree-ring standardization: defining the biological trend from expected basal area increment. Tree-Ring Res. 64, 81–96. https://doi.org/10.3959/2008-6.1.

Bogdziewicz, M., Kelly, D., Thomas, P.A., Lageard, J.G.A., Hacket-Pain, A., 2020. Climate warming disrupts mast seeding and its fitness benefits in European beech. Nat. Plants 6, 88–94. https://doi.org/10.1038/s41477-020-0592-8.

Breshears, D.D., Cobb, N.S., Rich, P.M., Price, K.P., Allen, C.D., Balice, R.G., Romme, W.H., Kastens, J.H., Floyd, M.L., Belnap, J., Anderson, J.J., Myers, O.B., Meyer, C.W., 2005. Regional vegetation die-off in response to global-change-type drought. Proc. Natl. Acad. Sci. U. S. A. 102, 15144–15148. https://doi.org/10.1073/pnas.0505734102.

Buma, B., 2015. Disturbance interactions: characterization, prediction, and the potential for cascading effects. Ecosphere 6, 1–15. https://doi.org/10.1890/ES15-00058.1.

Bunn, A., Korpela, M., Biondi, F., Campelo, F., Mérian, P., Qeadan, F., Zang, C., 2016. dplR: dendrochronology program library in R. R Package Version 1.6.4 Retrieved from. https://CRAN.R-project.org/package=dplR.

Burnham, K.P., Anderson, D.R., 2002. Model Selection and Multimodel Inference: a Practical Information-Theoretic Approach. 2nd Ed. vol. 60. Springer-Verlag, New York, USA.

Chmura, D.J., Rozkowski, R., 2002. Variability of beech provenances in spring and autumn phenology. Silvae Genet. 51, 123–127.

Clark, R.M., Thompson, R., 2010. Predicting the impact of global warming on the timing of spring flowering. Int. J. Climatol. 30, 1599–1613. https://doi.org/10.1002/joc.2004.

D'Andrea, E., Rezaie, N., Prislan, P., Gričar, J., Muhr, J., Collalti, A., Matteucci, G., 2020. Frost and drought: effects of extreme weather events on stem carbon dynamics in a Mediterranean beech forest. Plant Cell Environ. https://doi.org/10.1111/pce.13858.

Dantec, C.F., Vitasse, Y., Bonhomme, M., Louvet, J.M., Kremer, A., Delzon, S., 2014. Chilling and heat requirements for leaf unfolding in European beech and sessile oak populations at the southern limit of their distribution range. Int. J. Biometeorol. 58, 1853–1864. https://doi.org/10.1007/s00484-014-0787-7.

Davi, H., Gillmann, M., Ibanez, T., Cailleret, M., Bontemps, A., Fady, B., Lefèvre, F., 2011. Diversity of leaf unfolding dynamics among tree species: New insights from a study along an altitudinal gradient. Agric. For. Meteorol. 151, 1504–1513. https://doi.org/10.1016/j.agrformet.2011.06.008.

Di Filippo, A., Biondi, F., Čufar, K., De Luis, M., Grabner, M., Maugeri, M., Presutti Saba, E., Schirone, B., Piovesan, G., 2007. Bioclimatology of beech (*Fagus sylvatica* L.) in the Eastern Alps: spatial and altitudinal climatic signals identified through a tree-ring network. J. Biogeogr. 34, 1873–1892. https://doi.org/10.1111/j.1365-2699.2007.01747.x.

Di Filippo, A., Biondi, F., Maugeri, M., Schirone, B., Piovesan, G., 2012. Bioclimate and growth history affect beech lifespan in the Italian Alps and Apennines. Glob. Chang. Biol. 18, 960–972. https://doi.org/10.1111/j.1365-2486.2011.02617.x.

Dittmar, C., Fricke, W., Elling, W., 2006. Impact of late frost events on radial growth of common beech (*Fagus sylvatica* L.) in southern Germany. Eur. J. For. Res. 125, 249–259. https://doi.org/10.1007/s10342-005-0098-y.

Dormann, C.F., Elith, J., Bacher, S., Buchmann, C., Carl, G., Carré, G., García Marquéz, J.R., Gruber, B., Lafourcade, B., Leitão, P.J., Münkemüller, T., McClean, C., Osborne, P.E., Reineking, B., Chröder, B., Skidmore, A.K., Zurell, D., Lautenbach, S., 2013. Collinearity: a review of methods to deal with it and a simulation study evaluating their performance. Ecography 36, 27–46. https://doi.org/10.1111/j.1600-0587.2012.07348.x.

Easterling, D.R., Evans, J.L., Groisman, P.Y., Karl, T.R., Kunkel, K.E., Ambenje, P., 2000. Observed variability and trends in extreme climate events: a brief review. B. Am. Meteorol. Soc. 81, 417–425. https://doi.org/10.1175/1520-0477(2000)081<0417:OVATIE>2.3.CO;2.

Fu, Y.H., Piao, S., Op de Beeck, M., Cong, N., Zhao, H., Zhang, Y., Menzel, A., Janssens, I.A., 2014. Recent spring phenology shifts in western Central Europe based on multiscale observations. Glob. Ecol. Biogeogr. 23, 1255–1263. https://doi.org/10.1111/geb.12210.

Fu, Y.H., Zhao, H., Piao, S., Peaucelle, M., Peng, S., Zhou, G., Ciais, P., Huang, M., Menzel, A., Peñuelas, J., Song, Y., Vitasse, Y., Zeng, Z., Janssens, I.A., 2015. Declining global warming effects on the phenology of spring leaf unfolding. Nature 526, 104–107. https://doi.org/10.1038/nature15402.

Fu, Y.H., Zhang, X., Piao, S., Hao, F., Geng, X., Vitasse, Y., Zohner, C., Peñuelas, J., Janssens, I.A., 2019. Daylength helps temperate deciduous trees to leaf-out at the optimal time. Glob. Chang. Biol. 25, 2410–2418. https://doi.org/10.1111/gcb.14633.

Gazol, A., Camarero, J.J., Colangelo, M., de Luis, M., Martínez, E., del Castillo, E.M., Serra-Maluquer, X., 2019. Summer drought and spring frost, but not their interaction, constrain European beech and Silver fir growth in their southern distribution limits. Agric. For. Meteorol. 278, 107695. https://doi.org/10.1016/j.agrformet.2019.107695.

Giorgi, F., Lionello, P., 2008. Climate change projections for the Mediterranean region. Glob. Planet. Chang. 63, 90–104. https://doi.org/10.1016/j.gloplacha.2007.09.005.

Gordo, O., Sanz, J.J., 2009. Long-term temporal changes of plant phenology in the Western Mediterranean. Glob. Chang. Biol. 15, 1930–1948. https://doi.org/10.1111/j.1365-2486.2009.01851.x.

Guyon, D., Guillot, M., Vitasse, Y., Cardot, H., Hagolle, O., Delzon, S., Wigneron, J.P., 2011. Monitoring elevation variations in leaf phenology of deciduous broadleaf forests from SPOT/VEGETATION time-series. Remote Sens. Environ. 115, 615–627. https://doi.org/10.1016/j.rse.2010.10.006.

Hänninen, H., 1991. Does climatic warming increase the risk of frost damage in northern trees? Plant Cell Environ. 14, 449–454. https://doi.org/10.1111/j.1365-3040.1991.tb01514.x.

Haylock, M.R., Hofstra, N., Klein Tank, A.M.G., Klok, E.J., Jones, P.D., New, M., 2008. A European daily high-resolution gridded dataset of surface temperature and precipitation. J. Geophys. Res. 113, D20119. https://doi.org/10.1029/2008JD010201.

Holmes, R.L., 1983. Computer-assisted quality control in tree-ring dating and measurement. Tree Ring Bull 43, 69–78.

Hufkens, K., Friedl, M.A., Keenan, T.F., Sonnentag, O., Bailey, A., O'Keefe, J., Richardson, A.D., 2012. Ecological impacts of a widespread frost event following early spring leaf-out. Glob. Chang. Biol. 18, 2365–2377. https://doi.org/10.1111/j.1365-2486.2012.02712.x.

Inouye, D.W., 2000. The ecological and evolutionary significance of frost in the context of climate change. Ecol. Lett. 3, 457–463. https://doi.org/10.1046/j.1461-0248.2000.00165.x.

IPCC, Barros, V.R., Field, C.B., Dokken, D.J., Mastrandre, M.D., Mach, K.J., Bilir, T.E., ... White, L.L., 2014. Climate change 2014: impacts, adaptation, and vulnerability. Part B: Regional Aspects. Contribution of Working Group II to the Fifth Assessment Report of the Intergovernmental Panel on Climate Change. Cambridge University Press, Cambridge.

Jump, A.S., Hunt, J.M., Peñuelas, J., 2006. Rapid climate change-related growth decline at the southern range edge of *Fagus sylvatica*. Glob. Chang. Biol. 12, 2163–2174. https://doi.org/10.1111/j.1365-2486.2006.01250.x.

Kalberer, S.R., Wisniewski, M., Arora, R., 2006. Deacclimation and reacclimation of cold-hardy plants: current understanding and emerging concepts. Front. Plant Sci. 171, 3–16. https://doi.org/10.1016/j.plantsci.2006.02.013.

Kassambara, A., Mundt, F., 2016. Factoextra: extract and visualize the results of multivariate data analyses. Available at. https://CRAN.R-project.org/package=factoextra R Package Version 1.0.3.

Körner, C., Basler, D., Hoch, G., Kollas, C., Lenz, A., Randin, C.F., Vitasse, Y., Zimmermann, N.E., 2016. Where, why and how? Explaining the low-temperature range limits of temperate tree species. J. Ecol. 104, 1076–1088. https://doi.org/10.1111/1365-2745.12574.

Kramer, K., 1994. A modelling analysis of the effects of climatic warming on the probability of spring frost damage to tree species in the Netherlands and Germany. Plant Cell Environ. 17, 367–377. https://doi.org/10.1111/j.1365-3040.1994.tb00305.x.

Lasch-Born, P., Suckow, F., Gutsch, M., Hauf, Y., Hoffmann, P., Kollas, C., Reyer, C.P.O., 2018. Fire, late frost, nun moth and drought risks in Germany's forests under climate change. Meteorol. Z. 27, 135–148.

Lê, S., Josse, J., Husson, F., 2008. FactoMineR: a package for multivariate analysis. J. Stat. Softw. 258, 1–18. https://doi.org/10.18637/jss.v025.i01.

Lüdecke, D., Makowski, D., Waggoner, P., Patil, I., 2020. Package 'performance': assessment of regression models performance. R Package Version 0.4.5 Retrieved from. https://CRAN.R-project.org/package=performance.

van der Maaten-Theunissen, M., van der Maaten, E., Bouriaud, O., 2015. pointRes: an R package to analyze pointer years and components of resilience. Dendrochronologia 35, 34–38. https://doi.org/10.1016/j.dendro.2015.05.006.

Martinez del Castillo, E., Longares, L.A., Gričar, J., Prislan, P., Gil-Pelegrín, E., Čufar, K., de Luis, M., 2016. Living on the edge: contrasted wood-formation dynamics in *Fagus sylvatica* and *Pinus sylvestris* under Mediterranean conditions. Front. Plant Sci. 7, 370. https://doi.org/10.3389/fpls.2016.00370.

Menzel, A., Sparks, T.H., Estrella, N., Koch, E., Aasa, A., Ahas, R., Alm-Kübler, K., Bissolli, P., Braslavská, O., Briede, A., Chmielewski, F.M., Crepinsek, Z., Curnel, Y., Dahl, A., Defila, C., Donnelly, A., Filella, Y., Jatczak, K., Måge, F., Mestre, A., Nordli, Ø., Peñuelas, J., Pirinen, P., Remišová, V., Scheifinger, H., Striz, M., Susnik, A., Van Vliet, A.J.H., Wielgolaski, F.-E., Zach, S., Zust, A., 2006. European phenological response to climate change matches the warming pattern. Glob. Chang. Biol. 12, 1969–1976. https://doi.org/10.1111/j.1365-2486.2006.01193.x.

Menzel, A., Helm, R., Zang, C., 2015. Patterns of late spring frost leaf damage and recovery in a European beech (*Fagus sylvatica* L.) stand in South-Eastern Germany based on repeated digital photographs. Front. Plant Sci. 6, 1–13. https://doi.org/10.3389/fpls.2015.00110.

Miller, P., Lanier, W., Brandt, S., 2000. Using growing degree days to predict plant stages. 9. Montana State University Extension Service (MT00103 AG 7/2001). http://store.msuextension.org/publications/AgandNaturalResources/MT200103AG.pdf.

Muffler, L., Beierkuhnlein, C., Aas, G., Jentsch, A., Schweiger, A.H., Zohner, C., Kreyling, J., 2016. Distribution ranges and spring phenology explain late frost sensitivity in 170 woody plants from the northern hemisphere. Glob. Ecol. Biogeogr. 25, 1061–1071. https://doi.org/10.1111/geb.12466.

Muffler, L., Weigel, R., Hacket-Pain, A.J., Klisz, M., van der Maaten, E., Wilmking, M., Kreyling, J., van der Maaten-Theunissen, M., 2020. Lowest drought sensitivity and decreasing growth synchrony towards the dry distribution margin of European beech. J. Biogeogr. doi https://doi.org/10.1111/jbi.13884.

Nakagawa, S., Schielzeth, H., 2013. A general and simple method for obtaining R^2 from generalized linear mixed-effects models. Methods Ecol. Evol. 4, 133–142. https://doi.org/10.1111/j.2041-210x.2012.00261.x.

Olano, J.M., García-Cervigón, A.I., Sangüesa-Barreda, G., Rozas, V., Muñoz-Garachana, D., García-Hidalgo, M., García-Pedrero, A., 2021. Satellite data and machine learning reveal the incidence of late frost defoliations on Iberian beech forests. Ecol. Appl. doi https://doi.org/10.1002/eap.2288.

Peaucelle, M., Janssens, I.A., Stocker, B.D., Descals Ferrando, A., Fu, Y.H., Molowny-Horas, R., Ciais, P., Peñuelas, J., 2019. Spatial variance of spring phenology in temperate deciduous forests is constrained by background climatic conditions. Nat. Commun. 10, 5388. https://doi.org/10.1038/s41467-019-13365-1.

Peng, D., Wu, C., Li, C., Zhang, X., Liu, Z., Ye, H., Luo, S., Liu, X., Fang, B., 2017. Spring green-up phenology products derived from MODIS NDVI and EVI: Intercomparison, interpretation and validation using National Phenology Network and AmeriFlux observations. Ecol. Indic. 77, 323–336. https://doi.org/10.1016/j.ecolind.2017.02.024.

Peñuelas, J., Boada, M., 2003. A global change induced biome shift in Montseny mountains (NE Spain). Glob. Chang. Biol. 9, 131–140. https://doi.org/10.1046/j.1365-2486.2003.00566.x.

Pepin, N., Bradley, R.S., Diaz, H.F., Baraer, M., Caceres, E.B., Forsythe, N., Fowler, H., Greenwood, G., Hashmi, M.Z., Liu, X.D., Miller, J.R., Ning, L., Ohmura, A., Palazzi, E., Rangwala, I., Schöner, W., Severskiy, I., Shahgedanova, M., Wang, M.B., Williamson, S.N., Yang, D.Q., 2015. Elevation-dependent warming in mountain regions of the world. Nat. Clim. Chang. 5, 424–430. https://doi.org/10.1038/nclimate2563.

Pinheiro, J., Bates, D., DebRoy, S., Sarkar, D., 2014. Nlme: linear and nonlinear mixed effects models. R Package Version 3, 1–117.

Pinheiro, J.C., Bates, D.M., 2000. Mixed-Effects Models in S and S- PLUS. Springer-Verlag, New York, NY https://doi.org/10.1007/978-1-4419-0318-1.

Piovesan, G., 1998. Analisi di problemi assestamentali nella foresta montana dell'Appennino centrale. PhD Thesis. University of Tuscia, Viterbo (143pp).

Piovesan, G., 2019. A light-demanding pine spreads into a closed forest. Frontiers Ecol. Environ. 17, 454. https://doi.org/10.1002/fee.2109.

Piovesan, G., Adams, J.M., 2002. Masting behaviour in beech: linking reproduction and climatic variation. Can. J. Botany 79, 1039–1047. https://doi.org/10.1139/cjb-79-9-1039.

Piovesan, G., Bernabei, M., Di Filippo, A., Romagnoli, M., Schirone, B., 2003. A long-term tree ring beech chronology from a high-elevation old-growth forest of Central Italy. Dendrochronologia 21, 13–22. https://doi.org/10.1078/1125-7865-00036.

Piovesan, G., Biondi, F., Bernabei, M., Di Filippo, A., Schirone, B., 2005. Spatial and altitudinal bioclimatic zones of the Italian peninsula identified from a beech (*Fagus sylvatica* L.) tree-ring network. Acta Oecol. 27, 197–210. https://doi.org/10.1016/j.actao.2005.01.001.

Príncipe, A., van der Maaten, E., van der Maaten-Theunissen, M., Struwe, T., Wilmking, M., Kreyling, J., 2017. Low resistance but high resilience in growth of a major deciduous forest tree (*Fagus sylvatica* L.) in response to late spring frost in southern Germany. Trees 31, 743–751. https://doi.org/10.1007/s00468-016-1505-3.

Proietti, R., Antonucci, S., Monteverdi, M.C., Garfì, V., Marchetti, M., Plutino, M., Di Carlo, M., Germani, A., Santopuoli, G., Casteldi, C., Chiavetta, U., 2020. Monitoring spring phenology in Mediterranean beech populations through in situ observation and synthetic aperture radar methods. Remote Sens. Environ. 248, 111978. https://doi.org/10.1016/j.rse.2020.111978.

R Core Team, 2018. R: a language and environment for statistical computing. R Foundation for Statistical Computing. R Foundation for Statistical Computing, Vienna, Austria (Retrieved from). https://www.R-project.org/.

Rozas, V., Camarero, J.J., Sangüesa-Barreda, G., Souto, M., García-González, I., 2015. Summer drought and ENSO-related cloudiness distinctly drive *Fagus sylvatica* growth near the species rear-edge in northern Spain. Agric. For. Meteorol. 201, 153–164. https://doi.org/10.1016/j.agrformet.2014.11.012.

Salmela, M.J., Cavers, S., Cottrell, J.E., Iason, G.R., Ennos, R.A., 2013. Spring phenology shows genetic variation among and within populations in seedlings of Scots pine (*Pinus sylvestris* L.) in the Scottish Highlands. Plant Ecol. Divers. 6, 523–536. https://doi.org/10.1080/17550874.2013.795627.

Sangüesa-Barreda, G., Villalba, R., Rozas, V., Christie, D.A., Olano, J.M., 2019. Detecting *Nothofagus pumilio* growth reductions induced by past spring frosts at the northern Patagonian Andes. Frontiers Plant Sci. 10, 1413. https://doi.org/10.3389/fpls.2019.01413.

Scheifinger, H., Menzel, A., Koch, E., Peter, C., 2003. Trends of spring time frost events and phenological dates in Central Europe. Theor. Appl. Climatol. 74, 41–51. https://doi.org/10.1007/s00704-002-0704-6.

Schweingruber, F.H., Eckstein, D., Serre-Bachet, F., Bräker, O.U., 1990. Identification, presentation and interpretation of event years and pointer years in dendrochronology. Dendrochronologia 8, 9–38.

Serra-Maluquer, X., Gazol, A., Sangüesa-Barreda, G., Sánchez-Salguero, R., Rozas, V., Colangelo, M., Guitiérrez, E., Camarero, J.J., 2019. Geographically structured growth decline of rear-edge Iberian *Fagus sylvatica* forests after the 1980s shift toward a warmer climate. Ecosystems 22, 1325–1337. https://doi.org/10.1007/s10021-019-00339-z.

Stojnic, S., Sass-Klaassen, U., Orlovic, S., Matovic, B., Eilmann, B., 2013. Plastic growth response of European beech provenances to dry site conditions. IAWA J. 34, 475–484. https://doi.org/10.1163/22941932-00000038.

Stott, P., 2016. How climate change affects extreme weather events. Science 352, 1517–1518. https://doi.org/10.1126/science.aaf7271.

Testa, S., Soudani, K., Boschetti, L., Borgogno Mondino, E., 2018. MODIS-derived EVI, NDVI and WDRVI time series to estimate phenological metrics in French deciduous forests. Int. J. Appl. Earth. Obs. Geoinformation 64, 132–144. https://doi.org/10.1016/j.jag.2017.08.006.

Ummenhofer, C.C., Meehl, G.A., 2017. Extreme weather and climate events with ecological relevance: a review. Phil. Trans. R. Soc. B 372, 20160135. https://doi.org/10.1098/rstb.2016.0135.

Vanoni, M., Bugmann, H., Nötzli, M., Bigler, C., 2016. Drought and frost contribute to abrupt growth decreases before tree mortality in nine temperate tree species. Forest Ecol. Manag. 382, 51–63. https://doi.org/10.1016/j.foreco.2016.10.001.

Vitasse, Y., Basler, D., 2013. What role for photoperiod in the bud burst phenology of European beech. Eur. J. Forest Res. 132, 1–8. https://doi.org/10.1007/s10342-012-0661-2.

Vitasse, Y., Rebetez, M., 2018. Unprecedented risk of spring frost damage in Switzerland and Germany in 2017. Clim. Chang. 149, 233–246. https://doi.org/10.1007/s10584-018-2234-y.

Vitasse, Y., Schneider, L., Rixen, C., Christen, D., Rebetez, M., 2018. Increase in the risk of exposure of forest and fruit trees to spring frosts at higher elevations in Switzerland over the last four decades. Agric. For. Meteorol. 248, 60–69. https://doi.org/10.1016/j.agrformet.2017.09.005.

Vitasse, Y., Bottero, A., Cailleret, M., Bigler, C., Fonti, P., Gessler, A., Lévesque, M., Rohner, B., Weber, P., Rigling, A., Wohlgemuth, T., 2019. Contrasting resistance and resilience to extreme drought and late spring frost in five major European tree species. Glob. Chang. Biol. 25, 3781–3792. https://doi.org/10.1111/gcb.14803.

Vitra, A., Lenz, A., Vitasse, Y., 2017. Frost hardening and dehardening potential in temperate trees from winter to budburst. New Phytol. 216, 113–123. https://doi.org/10.1111/nph.14698.

Weigel, R., Muffler, L., Klisz, M., Kreyling, J., van der Maaten-Theunissen, M., Wilmking, M., van der Maaten, E., 2018. Winter matters: sensitivity to winter climate and cold events increases towards the cold distribution margin of European beech (*Fagus sylvatica* L.). J. Biogeogr. 45, 2779–2790. https://doi.org/10.1111/jbi.13444.

Zimmermann, N.E., Yoccoz, N.G., Edwards, T.C., Meier, E.S., Thuiller, W., Guisan, A., Schmatz, D.R., Pearman, P.B., 2009. Climatic extremes improve predictions of spatial patterns of tree species. P. Nat. Acad. Sci. USA 106, 19723–19728. https://doi.org/10.1073/pnas.0901643106.

Zohner, C.M., Mo, L., Renner, S.S., Svenning, J.C., Vitasse, Y., Benito, B.M., Ordonez, A., Baumgarten, F., Bastin, J.-F., Sebald, V., Reich, P.B., Liang, J., Nabuurs, G.-J., de Miguel, S., Alberti, G., Antón-Fernández, C., Balazy, R., Brändli, U.-B., Chen, H.Y.H., Chishom, C., Cienciala, E., Dayanandan, S., Fayle, T.M., Frizzera, L., Gianelle, D., Jagodzinski, A.M., Jaroszewicz, M., Jucker, T., Kepfer-Rojas, S., Latif Khan, M., Kim, H.S., Korjus, H., Johannsen, V.K., Laarmann, D., Lang, M., Zawila-Niedzwiecki, T., Niklaus, P.A., Paquette, A., Pretzsch, H., Saikia, P., Schall, P., Šebeň, V., Svoboda, M., Tikhonova, E., Viana, H., Zhang, C., Zhao, X., Crowther, T.W., 2020. Late-spring frost risk between 1959 and 2017 decreased in North America but increased in Europe. P. Nat. Acad. Sci. USA 117, 12092–12200. https://doi.org/10.1073/pnas.1920816117.

Zuur, A.F., Ieno, E.N., Walker, N., Saveliev, A.A., Smith, G.M., 2009. Mixed Effects Models and Extensions in Ecology with R (New York).